Periodica Polytechnica
Mechanical Engineering

58(2), pp. 83-86, 2014
DOI:10.3311/PPme.7124

RESEARCH ARTICLE

Increase of load bearing capacity of a square-form nanofilter

Ádám Kovács, *Andras* Kovacs

RECEIVED 19 OCTOBER 2013; ACCEPTED AFTER REVISION 9 APRIL 2014

Abstract

Square-form, multi-layered nanofilter membranes have been investigated experimentally and by numerical simulation to determine their load bearing capacity versus filtration ability. The effect of various topologies combining the thickness of a load-carrying layer and Si-reinforcement on the bursting pressure has been determined. Based upon the comparison of a performance index an optimal structure could be selected for later production.

Keywords

nanofiltration · multi-layered membrane · porous structure

Ádám Kovács
Department of Applied Mechanics, Faculty of Mechanical Engineering,
Budapest University of Technology and Economics,
Műegyetem rkp. 3., H-1111 Budapest, Hungary
e-mail: adamo@mm.bme.hu

Andras Kovacs
Faculty of Computer and Electrical Engineering, Furtwangen University,
Robert-Gerwig-Platz 1, 78120 Furtwangen, Germany
e-mail: kovacs@hs-furtwangen.de

1 Introduction

Porous silicon is found in many applications, e.g. sensors, tissue engineering, medical therapeutics and diagnostics, photovoltage, rechargeable batteries, energetic materials, photonics and also in micro-electromechanical systems (MEMS) [1]. Depending on the pore sizes its structure can serve for filtration purposes from nano- to microfiltration. The filtration capacity depends mostly on the porosity, which – unfortunately – diminishes the strength, and consequently, the load bearing capacity of the system. Several reinforcement solutions are known to increase the bursting (critical) pressure of the structure, e.g. built-in extra layer having high strength (e.g. silicon-nitride, SiN), single-crystal silicon (cSi) columns, or the combination of them.

The investigated membranes are square-formed, made from a very thin perforated silicon-nitride (SiN) layer on a much thicker porous silicon (PS) layer, which is supported and reinforced by single-crystal silicon (c-Si) columns (Fig. 1).

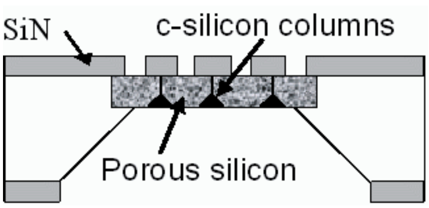

Fig. 1. Sketch of porous nanofilter

The figure is not scaled, it only shows the structure of the filter membrane. Since this base structure is fabricated by a wet etching technology from a thick wafer, a very stiff thick silicon frame remains around the membrane.

Three main types of configuration have been fabricated, assigned by A, B and C (Fig. 2). In order to obtain higher filtration rate the porosity should be as high as possible which diminishes the strength, and consequently, the load capacity of the device. This effect can be compensated by application of thicker SiN support layer and/or cSi-columns as a support grid within the PS-layer.

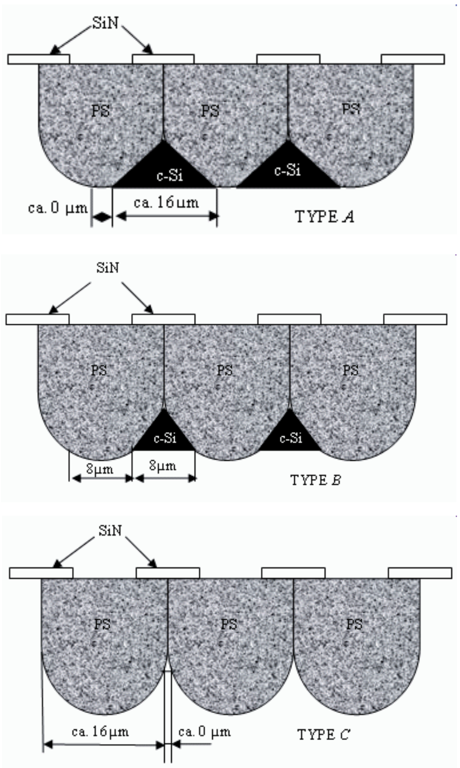

Fig. 2. Test structure configurations

All three types have an upper thin SiN-layer, and a thick PS-layer. Changes are made by depositing extra cSi-reinforcement of different amount (Types *A* and *B*), as well as by changing the porosity and the thickness of the layers within one type.

Silicon and silicon-nitride are commonly considered as brittle elastic materials, therefore their two fundamental material parameters corresponding to strength and load bearing capacity are the elastic modulus and the fracture strength. The higher the porosity is, the less is the elastic modulus of the structure. On the other hand, the load bearing capacity can directly be characterized by the bursting pressure, which determines the fracture strength of the material. For high filtration large porosity is required; however, a good load bearing capacity is also desirable. Since porosity and large fracture strength contradict each other, one should find an optimal configuration. This optimum can be searched for by creating a performance index *f*, which is simply defined as a rate of the fracture strength (σ_B) and the elastic modulus (E). Largest value of this index shows the optimum.

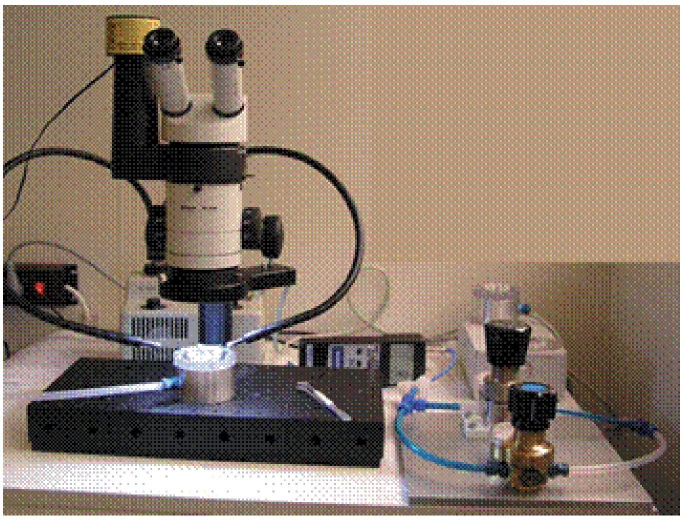

Fig. 3. Measurement set-up

2 Experimental work

The experimental set-up (Fig. 3) consists of a pressure box, where the test structure was put, a microscope and a camera.

The maximum deflection of the samples made from the base materials (cSi, SiN) has been detected by a computer connected to the camera, while the bursting pressure was registered by another computer connected to the manometer between the air-pressure control unit and the pressure box (Fig. 4).

Elastic moduli of the base materials have been determined analytically from the measured middle-point deflection using the elastic thin plate theory [2]. The effective elastic modulus needed for the performance index of the whole membrane was then calculated by a simple averaging method [3] from the elastic moduli of the upper layer and the cSi-reinforcement. The elastic modulus of the porous silicon layer was detemined by the simple formula

$$E_p = (1 - P)E$$

suggested by van Rijn [4], where P is the porosity rate.

Fracture strength was calculated by using the maximum normal stress theory commonly applied for brittle materials:

$$\sigma_f = |\sigma_1|_{\max}$$

where σ_1 is the maximum principal stress in the plate. Similarly to the calculation of E, an analytical estimate has been made for the relationship between the measured bursting pressure p_{crit} and σ_1 [2].

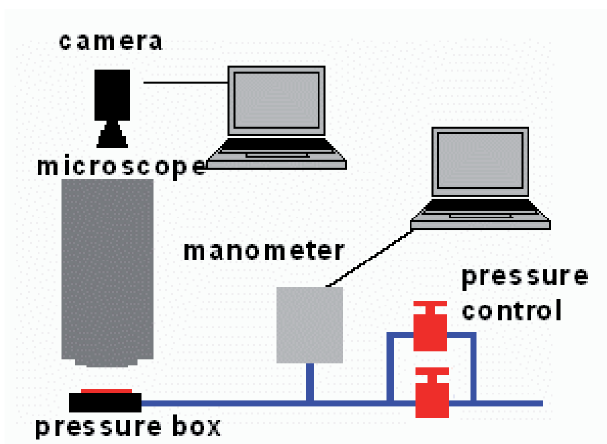

Fig. 4. Scheme of the experimental set-up

3 Results and discussion

A series of seven different structures have been produced from the three major types (Table 1).

Tab. 1. Geometrical parameters of test structures

	A	B1	B2	B3
L (µm)	1500	1000	1500	1500
h_SiN (µm)	0,085	0,050	0,050	0,050
h_PS (µm)	23	25	27	20
	C1	**C2**	**C3**	
L (µm)	1500	1000	1000	
h_SiN (µm)	0,052	0,051	0,052	
h_PS (µm)	21	20	29	

One specimen was produced from Type *A* structure, 3-3 pieces from Types *B* and *C*. They differed in the side-length of the square plate (*L*), and the thicknesses of the upper SiN (*h_SiN*) and the porous silicon layer (*h_PS*), respectively. The thickness values are rounded to thousandts.

Figure 5 shows the variation of the calculated elasticity modulus versus the the applied pressure in the case of the B1 structure.

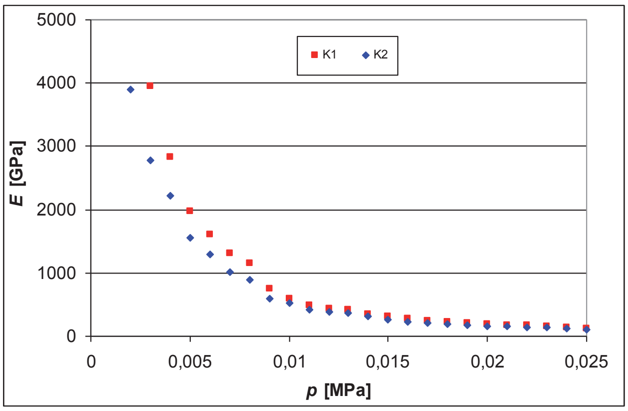

Fig. 5. Change of estimated elasticity modulus vs. applied pressure (B1 structure) – total pressure range

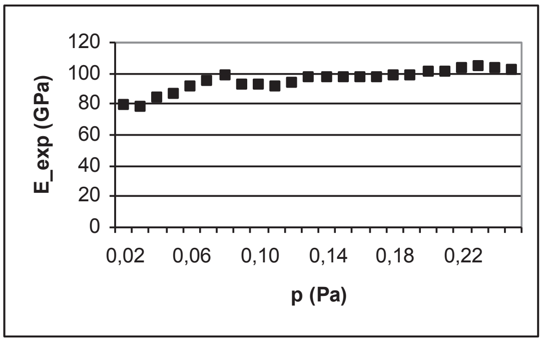

Fig. 6. Change of estimated elasticity modulus vs. applied pressure (B1 structure) – high pressure range

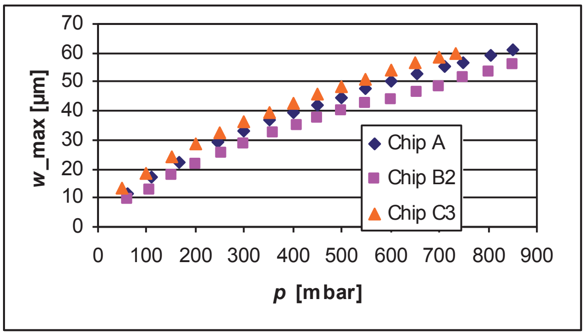

Fig. 7. Variation of the maximum deflection of the membrane vs. applied pressure

It is clearly seen in Fig. 5 that a minimum pressure should be applied to obtain a stable material parameter. This can be explained by the uncertain measurement at very low pressure. Zooming-in to the right-hand part of the diagram the value of *E* becomes almost constant (Fig. 6), which proves this statement.

Similar feature have been experienced in the case of all other structures.

Figure 7 shows the maximum deflection of the membrane as a function of the applied pressure for three typical structures (*A*, *B2* and *C3*).

The last points in the graphs represent the bursting pressures of the chips. The diagram shows a slightly nonlinearity between w_{max} and p, which is due to perforation of the upper layer. This nonlinearity has been already reported in [5].

Table 2 summarizes the numerical results for the calculated material parameters, as well as the performance indeces.

Tab. 2. Calculated material parameters and performance indeces

	A	B1	B2	B3
E [GPa]	14.63	10.69	10.83	11.87
σ_B [MPa]	303.9	280.1	278.0	287.2
$f = \sigma_B / E$	0.0208	0.0262	0.0257	0.0242
	C1	**C2**	**C3**	
E [GPa]	5.94	5.94	5.87	
σ_B [MPa]	251.4	251.5	251.0	
$f = \sigma_B / E$	0.0423	0.0423	0.0428	

These results show that although structures of Type *C* do not contain added cSi-reinforcement, and consequently, their fracture strengths are much less, than those of the other two chip types, the resulting softness is compensated by much higher filtration ability. The applicability of this structure type highly depends on the working pressure of the filtered medium. If the pressure could be kept under 700 mbar (see Fig. 7), Type *C* would be chosen as optimum. For this type of structures the performance index is almost constant, which demonstrates the importance of the upper SiN-layer. The side length of the membrane and the thickness of the porous layer played much less role in the results.

4 Conclusions

The key issue in assessment of applicabilty of multi-layered micro or nanofilters is the determination of their elasticity modulus and fracture strength. Once we know them, the performance index helps us to choose the optimal design. In order to get stable *E*-values, the test pressure must exceed the minimum pressure. In our experiments this was about 60 mPa.

The ultimate strength can be determined from the bursting (critical) pressure, which is the principal quantity of load bearing capacity.

The presence of single crystal reinforcement columns leads to a clear decrease of maximum deflection (~ $1/E$) and maximum normal stress (~ $1/p_{crit}$). The fracture strength is mainly affected by the thickness of the upper silicon-nitride layer and is hardly modified by the thickness of the porous silicon layer. Among the pre-concepts of design, the structure of Type *C* showed the best performance index.

References

1 **Sailor M. J.**, *Porous Silicon in Practice.* Wiley-VCH Verlag (2011).

2 **Kovács Á., Kovács A., Mescheder U.**, *Estimation of elasticity modulus and fracture strength of thin perforated SiN membranes with finite element simulations*. Computational Materials Science, 43 (1), pp. 59-64, (2008). DOI: 10.1016/j.commatsci.2007.07.023

3 **Kovács Á., Kovacs A.**, *Effect of silicon reinforcement on load-capacity of porous nanofilters*. Proceedings in Applied Mathematics and Mechanics, 8 (1), pp. 10215-10216, (2008). DOI: 10.1002/pamm.200810215

4 **van Rijn C. J. M.**, *Nano and Micro Engineered Membrane Technology*. Elsevier, Amsterdam (2004).

5 **Kovács A., Kovacs Á., Pogány M., Mescheder U.**, *Mechanical investigation of perforated and porous membranes for micro- and nanofilter applications*. Sensors and Actuators B: Chemical, 127 (1), pp. 120-125, (2007). DOI: 10.1016/j.snb.2007.07.044